P14.22

Rain heterogeneity studies and specific Z-R relationships determination with x-band and k-band radars to improve rain rate retrieval.

Frédéric TRIDON, Joël VAN BAELEN*, and Yves POINTIN

Laboratoire de Météorologie Physique (LaMP),
CNRS / Université Blaise Pascal Clermont-Ferrand II
24, avenue des Landais, 63177 Aubière cedex, France
Email: F.Tridon@opgc.univ-bpclermont.fr

ABSTRACT

In this work, we use the combination of an X-band high time and spatial resolution local area weather radar (typically 30 seconds in time and 60 meters in range and 2° in azimuth up to 20 kilometers) and a K-band vertically looking Micro Rain Radar to study the temporal and spatial heterogeneity of rain and its corresponding drop size distribution within precipitating systems. Then, defining simple classification criteria (based on rain intensity, trend, time variability, etc...), we determine separate rain regimes for which we can derive specific Z-R relationships. Applying these relationships to the X band reflectivity measurements allows us to improve rain rate restitutions over the size of a small urban basin after adequate correction for the attenuation effects.

INTRODUCTION

During more than 50 years of development, ground-based weather radars have become a research and operational tool well suited for precipitation surveillance and, eventually, quantitative rainfall measurements. The major source of errors lies in the conversion of the radar reflectivity factor Z (mm^6 m^{-3}) to rain rate R (mm h^{-1}). These two parameters are related to each other via the raindrop size distribution (DSD) which cannot be inferred by conventional weather radar measurements. Hence, it has been common practice to take a simple power law relationship between Z and R, like the well known Marshall-Palmer relationship. However, DSD is extremely variable in time and space even within a single precipitating event. Thus, many of these relationships have been proposed, nevertheless, in most of the cases, a unique relationship is used for one precipitating event.

The aim of this work is to categorize the different rain regimes that might occur even within individual precipitation cells to derive the corresponding specific relationships. Then we will confront the rain estimates with these specific relationships to the classical approach using one single relationship in order to investigate their potential for improve rain estimation. To do so, we analyse the simultaneous measurements of a scanning X-band radar and a vertically pointing K-band radar in their common volume.

In section 2, we will describe the radars and data. In section 3, we will present the methods and their performances. Finally, we will outline some conclusions and perspective for future developments.

EXPERIMENTAL SET-UP

During the summer of 2007, for the international COPS campaign (Convective and Orographically induced Precipitations Study, Wulfmeyer et al., 2008), the X-band radar was installed on a small hill at the foot of the Vosges mountains in order to overlook a largely instrumented site where we had installed the K-band radar, but also to monitor

the convective initiation activity over the transition area from the crest of the Vosges to the plains of the Rhine (see also Hagen et al, this issue).

The X-band (9.41 GHz) radar is a small low cost navigation system modified to be capable of precipitation measurements. Its main characteristics are its high time and space resolution: 30 s in time, 60 m in range up to a maximum range of 20 km, and 2° in azimuth with a beam width of 2.4°. For scanning operations, the radar beam elevation is fixed but can be set to any angle between 2° and 20° while the antenna rotates at a fixed rate of 24 rpm. Pictures of the radar and its operational configuration as well as a measurement example are shown in Figure 1.

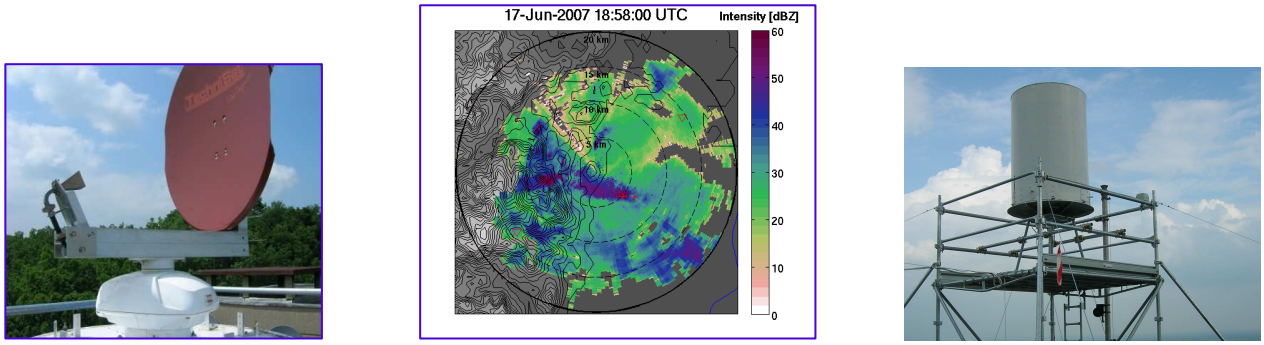

Figure 1: (a) Details of the radar base and its parabola set-up, (b) PPI example, (c) Field deployement set-up with radome in place.

The K-band (24.15 GHz) radar is a Micro Rain Radar (MRR): it is a FMCW system which provides Doppler spectra with 64 bins covering a range of 0.8 to 12.2 m/s over 30 range gates of 100 m with a typical time resolution of 10 s. Under the assumption of zero vertical wind, the profiles of DSD are derived using the relation between the drop diameters and their terminal fall velocity (Atlas et al., 1973). These profiles of DSD allow to correct for the rain attenuation, and to derive reflectivity factor and rain rate. Further details are described in Peters et al., 2005. Figure 2 shows examples of the MRR DSD profiles, as well as time series of radar reflectivity and rain rate.

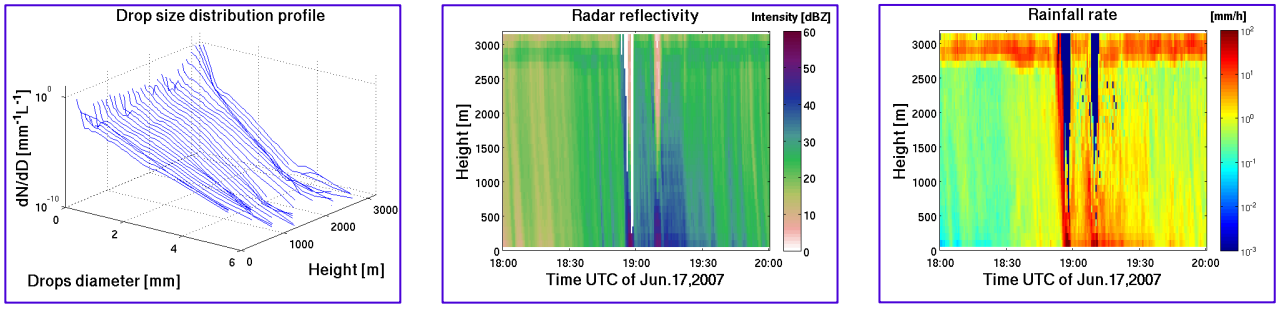

Figure 2: (a) Profile of MRR retrieved DSD, (b) Time series of radar reflectivity, (c) Time series of rain rate.

The set up of the two radars (X band and MRR) is such that at each scan their beams intersect (see Figure 3a). An example of the resulting reflectivity measured by the two systems in their common volume sounded during the night of August 07, 2007, is presented in Figure 3b. The reflectivity time series correspond very well and show very

similar features. However, one can notice slight differences which could be attributed to the differences between the sampling strategies and the two volumes sounded by the radars. Indeed, the geometrical dimensions of the radar beams are noticeably different with a volume ratio close to 100 (see Figure 3a). Thus, the X-band radar volume can include parts of the precipitating system not seen by the MRR. Furthermore, attenuation correction was also taken into account by applying the classical Hitschfeld and Bordan (1953) method to the X-band radar reflectivity measurements (Figure 3c). Finally, we performed a statistical cross calibration between the X-band and MRR reflectivity which allows a relative comparison of rain rate between the two systems.

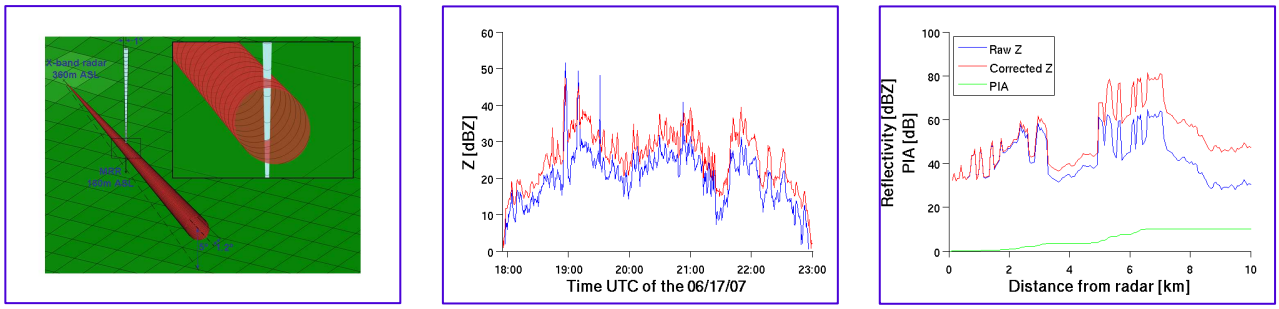

Figure 3: (a) Geometry of the intersection of the two radar beams, (b) Reflectivity time series examples, (c) X band radar attenuation correction.

RAIN REGIMES CLASSIFICATION AND PRECIPITATION ESTIMATION

We will now consider the observations from the two radars in the common volume in order to investigate the Z-R relationships to be applied to the X-band reflectivity field. Our objective is to use the MRR measurements to help us find simple techniques to categorize rain regimes from the X-band reflectivity. We propose different schemes based on the trend of this reflectivity intensity (increasing, decreasing, stagnating) or on its intensity itself.

The MRR measured reflectivity and estimated rain-rate are used to derive the corresponding Z-R relationship which is then applied to the X-band radar reflectivity measurements in order to calculate a corresponding rain-rate which, in turn, is compared to the MRR derived value. This procedure is biased towards the MRR estimation which we will use as a reference, but the goal at this point of the project is to evaluate candidate rain regime selection scheme to later improve rainfall estimates.

Figure 4a shows the two radar reflectivity time series measured in the common volume after cross-calibration of the two systems and attenuation correction applied to the X band measurements: they definitely show very similar features. Then we determine the mean Z-R relationship from MRR measurements in the common volume to estimate the precipitation from the X-band radar reflectivity (Figure 4b) and finally we determine the corresponding mean DSD for the MRR sounded volume.

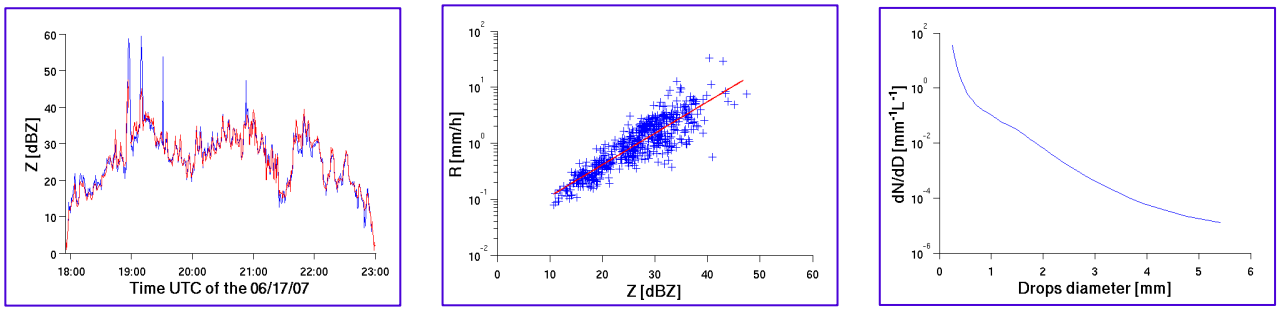

Figure 4: (a) X band and MRR reflectivity time series in common volume, (b) MRR derived mean Z-R relationship, (c) corresponding DSD

The following step is then to apply simple selection criteria in order to classify different rain regimes and determine their specific Z-R relationships. The first scheme is based on the intuitive fact that bigger drops are perceived when rain intensifies, while only smaller drops are left when rain decreases in intensity. The second scheme considers only the rain intensity itself, classifying the rain into low, medium and strong rain intensity categories. Finally we have also considered the statistical method proposed by Clemens et al. where extended periods of "coherent rain structures" corresponding to a single Z-R relationship are identified but it could only apply on individual events as every identified period is associated to a distinct relationship and can thus only account for parts of the rain event.

For example, Figure 5 shows the results for the increasing, stagnating and decreasing rain intensity classification scheme. Panel (a) shows the reflectivity time series with the different "sections" identified. Panel (b) shows the corresponding DSD which demonstrate that the increasing intensity periods are indeed associated with more and larger drops. Panel (c) shows the corresponding Z-R relationships and their associated clouds of points.

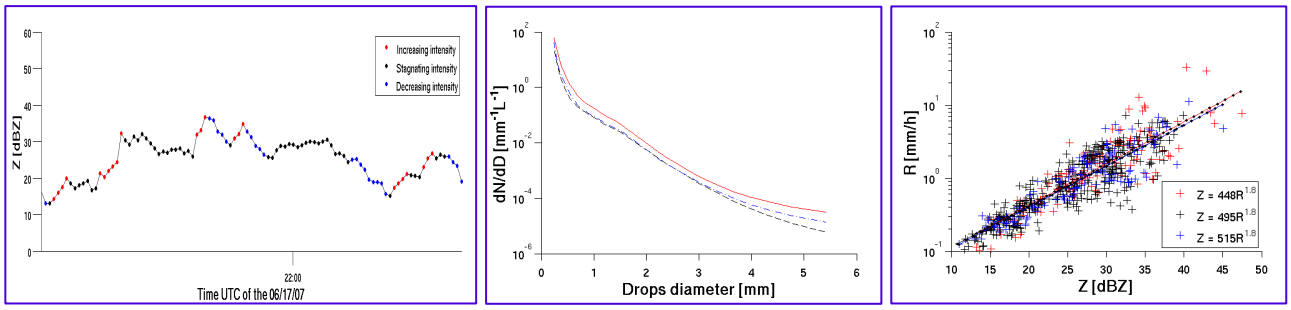

Figure 5: (a) reflectivity time series with rain categories identified, (b) corresponding DSD's, (c) Z-R space and the rain categories corresponding Z-R relationships.

The different classification schemes have been applied to the whole data set of COPS campaign (i.e., that is about 100 hours of measurements corresponding to 25 events of various precipitation types from stratiform to convective rain). Applying the different methods to all the separate events individually generally leads to slight improvements over the MRR estimates taken as a reference in this case, as shown in Table 1. In particular, the rain trend methods using three categories of increasing, stagnating, and decreasing rain intensity gives excellent results when compared to a single "global" relationship. On the other hand, the rain intensity classification does not provide benefits but we

could trace this problem to the fact that the highest rain intensity category had only few points to account for and, hence, could lead to sometimes erroneous estimations which have a strong impact on the final result. Finally, the statistical methods is efficient but can only apply to about half of the rain periods observed.

Total rainfall	MRR	Global Z-R	Adapted Z-R
Increasing, stagnating and decreasing	73,51	71,45 (-2,80%)	73,27 (-0,33%)
Increasing and decreasing	73,51	71,45 (-2,80%)	71,48 (-2,76%)
Rain intensity	73,51	71,45 (-2,80%)	68,71 (-6,53%)
Statistical	36,36	31,67 (-12,90%)	33,50 (-7,87%)

Table 1: Results for the different classification schemes applied to the individual events summed together and compared to the MRR estimates

We have also applied the classification scheme over the entire campaign in order to check if there could be a single category wide relationship which would provide improvements over a global law (itself already different and better adapted to the measurements than the classical Marshall-Palmer (1948) relationship). That is summarized in Table 2. In this case the rain trend classification scheme still provides benefits.

Total rainfall	MRR	Global Z-R	Adapted Z-R
Increasing, stagnating and decreasing	76,47	73,51 (-3,90%)	74,06 (-3,15%)
Increasing and decreasing	76,47	73,51 (-3,90%)	73,24 (-4,22%)
Rain intensity	76,47	73,51 (-3,90%)	66,31 (-13,30%)
Statistical	-	-	-

Table 2: Results for the different classification schemes applied to the entire campaign and compared to the MRR estimates

CONCLUSIONS AND PERSPECTIVES

We have shown the need in using specific Z-R relationships to account for the high variability of rain regimes within the precipitations systems. To determine these specific Z-R relationships, the classification scheme based on the trend of the reflectivity intensity (increasing, stagnating, decreasing) shows good promises for improvement of the rain estimation. However, the selection scheme can still be refined, while we consider also the possibility to combine different classification schemes.

Finally, we are still working on the amelioration of this classification scheme in order to extend the application of the specific relationships retrieved to the entire X band radar domain and to validate this study by

rainfall comparisons with a network of raingages over the domain covered by the X-band radar.

REFERENCES

Atlas, D., Srivastava R. and Sekhon R., 1973: Doppler radar characteristics of precipitation at vertical incidence, *Rev. Geophys. Space Phys*., **11**, 1-35.

Clemens, M., G. Peters, J. Seltmann, and P. Winkler, 2008, Identification of temporal constant Z-R relationships based on measurements using Micro rain radars, International Conference on Weather Radar in Hydrology, Grenoble, France, 10-12 March.

Hitschfeld, W., and Bordan, J.; 1953: Errors inherent in the radar measurements of rainfall at attenuation wavelengths, *J. Meteor*., **11**, 58--67.

Marshall, J.S., and W.M. Palmer, 1948: The distribution of raindrops with size, *J. Meteor*., 5, 165-166.

Peters, G., B. Fischer, H. Münster, M. Clemens, A. Wagner, 2005: Profiles of Raindrop Size Distributions as Retrieved by Micro Rain Radars, *J. Appl. Meteorol*., **44**, 1930-1949.

Wulfmeyer, V., A. Behrendt, H.-S. Bauer, C. Kottmeier, U. Corsmeier, A. Blyth, G. Craig, U. Schumann, M. Hagen, S. Crewell, P. Di Girolamo, C. Flamant, M. Miller, A. Montani, S. Mobbs, E. Richard, M.W. Rotach, M. Arpagaus, H. Russchenberg, P. Schlüssel, M. König,, V. Gärtner, R. Steinacker, M. Dorninger, D.D. Turner, T. Weckwerth, A. Hense, and C. Simmer, 2008: The Convective and Orographically-induced Precipitation Study: A Research and Development Project of the World Weather Research Program for improving quantitative precipitation forecasting in low-mountain regions. *Bull. Amer. Meteor. Soc.*, **89** (10), 1477-1486, DOI:10.1175/2008BAMS2367.1.